

**Direct observation of a precursor in a complex system**

R. L. Santos and J. M. A. Figueiredo\*

*Departamento de Física, Universidade Federal de Minas Gerais, Caixa Postal 702, Belo Horizonte, CEP 31.270-901, Brazil*

(Received 23 March 2006; published 3 October 2006)

A precursor is a kind of instability in a nonequilibrium system observed prior to a bifurcation. It has been observed in important natural phenomena such as earthquakes and epileptic seizures. In most cases just qualitative results were reported, with the exception of some quantitative observations of noisy precursors. We report the observation of precursors excited by a deterministic perturbation. Quantitative characterization of this type of precursor is important in predicting a bifurcation in advance. This predicting ability comes from a dynamical structure present on the perturbed system.

DOI: [10.1103/PhysRevE.74.041104](https://doi.org/10.1103/PhysRevE.74.041104)

PACS number(s): 05.70.Ln, 47.20.Ky, 47.54.-r

A macroscopic system operating out of its equilibrium state may exist in a variety of states called branches. Non-linear interactions of the thermodynamic fields that define a branch may produce qualitative changes on its properties and may lead to the emergence of self-organized structures. In such cases other stable regimes may be attained which present spatiotemporal patterns. This is the case when a spontaneous symmetry breaking, at a bifurcation point, drives a high symmetric state, like a uniform pattern, into a branch with lower symmetry presenting, for example, a periodic structure. An important challenge in the study of these nonlinear dynamic systems is the detection of whether a bifurcation belongs to a specific stable branch. In this respect, nontrivial effects may appear in a system when a stable branch, subject to a perturbation, presents dynamical structure not observed before the perturbation is set on. Therefore, the study of a perturbed branch may be of importance in providing in advance information concerning the existence of a bifurcation in that branch. When this happens, a precursor is observed. Pioneering work on this matter was reported by Wiesenfeld [1]. He studied a nonlinear system existing in a periodic state and subject to an external noise source and predicted that, prior to an instability, the power spectra of the primary signal may anticipate the kind of bifurcation that will be triggered.

Since then experimental evidence of precursors was reported in widely different fields. A program using geophysical data to predict earthquakes has been implemented by Wyss [2,3] and correlation of direct data on seismic activity and electromagnetic anomalies were used by Eftaxias *et al.* [4] in order to demonstrate that existing methods of data analysis are quite reliable in making predictions. The importance of reliable and robust detection of precursors of epileptic seizures has been recognized as a factor of life improvement in epilepsy sufferers [5]. In this respect, analysis of electroencephalogram (EEG) signals was used by Martinerie *et al.* [6], who performed multidimensional data analysis in order to predict the onset of epileptic seizures. Similar conclusions were reported by Lehnertz and Elger [7] showing that nonlinear time-series analysis are capable of extracting relevant features of brain activity which are predictive of

epileptic seizures. Noise precursors of the type predicted by Wiesenfeld were observed in semiconductor junctions [8], laser instabilities [9] and Josephson junctions [10,11]. Prebifurcation studies of noise-driven systems were also performed by Surovyatkina and Kravtsov [12,13].

In this work, we report a direct observation of a kind of precursor, not related to noise coupling excitations but induced by coupling of the intrinsic dynamics of a controlled system with a deterministic perturbation. More specifically, our system exhibits a spatial pattern formation by means of a spontaneous symmetry breaking of a uniform pattern, after a supercritical pitchfork bifurcation. The imposed perturbation changes a parameter that affects this stable branch. We were able to detect the presence of precursor in this case. Detailed observations of the evolution of precursor modes across a wide range of the control parameter were made, including those values that were very close to the bifurcation point. Our data suggest that a precursor regime may be defined through the existence of an interval of control parameter values where precursors are present. In this sense, two kinds of regimes were observed and characterized. In addition, post-bifurcation effects were also observed and they showed that a strong interaction of precursor modes with spatial pattern modes, set after the bifurcation point, is present. Our data also shows a suppression of these excited precursor modes whenever the system operates far from the bifurcation point.

The experimental setup for the kind of pattern instability we worked out consists of a rotating cylinder, partially immersed in a fluid, and placed over a horizontal plate, as used by Hakim *et al.* in Ref. [14] and shown in Fig. 1. Within these conditions, a one-dimensional straight interface (the uniform prebifurcation pattern) between the fluid and the open atmosphere is formed. When the angular frequency of the cylinder reaches a critical value,  $\omega_c$ , the interface presents a periodic spatial pattern. This instability was originally described by Pitts and Greiller [15] in a journal-bearing geometry. Linear stability analysis for this bifurcation was performed by Hakim *et al.* [14] and phase space domains reported by Rabaud *et al.* [16] for an experiment in a similar geometry. Secondary instabilities were reported by Cummins *et al.* [17]. In our experiment, the cylinder is a stainless steel shaft driven by a precision dc motor and mounted on aligned bearings. The shaft rotates immersed in a flat reservoir containing silicon oil. Parallelism between the cylinder axis and the horizontal base of the reservoir is adjusted by supporting

\*Electronic address: josef@fisica.ufmg.br

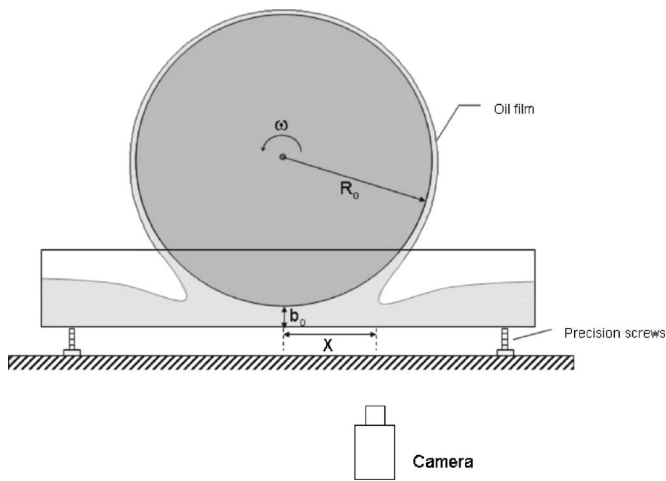


FIG. 1. Sketch of the experimental setup. The cylinder was adjusted at three distances to the plate,  $b_o=300 \mu\text{m}$  ( $\omega_c=2.53 \text{ rad/s}$ ),  $b_o=400 \mu\text{m}$  ( $\omega_c=4.8 \text{ rad/s}$ ), and  $b_o=800 \mu\text{m}$  ( $\omega_c=11.58 \text{ rad/s}$ ).

precision screws. The cylinder has a radius of 31.3 mm, length of 250.0 mm and eccentricity,  $\epsilon \approx 10 \mu\text{m}$ . In the experiments, variations in the control parameter were achieved by changing the angular frequency of the cylinder at three different distances ( $b_o$ ) between the cylinder and the plate. Liquid fluid used is a silicon oil (Dow Corning 200) of viscosity,  $\mu$ , equal to  $4.80 \times 10^{-2} \text{ Kg m}^{-1} \text{ s}^{-1}$  and having surface tension,  $T$ , equal to  $2.08 \times 10^{-2} \text{ N m}^{-1}$ , both specified at  $25 \text{ }^\circ\text{C}$ . For better stability of these parameters, room temperature was constantly maintained within  $\pm 0.5 \text{ }^\circ\text{C}$ .

For a given set of parameters, several sequences of images of the interface were obtained by using an asynchronous mode digital CCD camera. This technique allows a better compromise between pixel window and scan rate, with maximum time resolution. In all experiments we set the frame rate to  $16.4 \text{ s}^{-1}$ . Interface motion was recorded during a time interval covering not less than 50 times the period of one turn. A spatial resolution of  $68 \mu\text{m}$  was adjusted in order to permit a spatial window sufficient for observation of the interface instability. Acquired digital images were processed by using a computer program we developed employing edge detection techniques. The arithmetic mean of pixel data extracted from a specific frame was used to define interface position. We also wrote a computer code that calculated the Fourier transform of the obtained interface positions in time. The range of angular frequencies of the rotating cylinder was chosen in order to get a clear observation of the interface dynamics at both pre- and post-bifurcation branches. A typical image of the interface in these two cases is displayed in Fig. 2. In the prebifurcation branch, shown in Fig. 2(a), the interface is in a state that possesses high spatial symmetry, presenting the observed straight morphology. In Fig. 2(b), the interface is observed in a lower spatial symmetry branch, presenting a periodic morphology. For a given distance  $b_o$  and angular frequency,  $\omega$ , the interface experiences a recoil due to wetting effects as well as to the hydrodynamic equilibrium involving pressure and velocity fields. In order to determine specific parameters for this system, the mean position of the interface obtained from an average of its pixel



FIG. 2. Images of the straight morphology (a) observed in the prebifurcation branch and pattern-forming (b) present in the post-bifurcation branch. In both images the air is located above the interface and silicon oil is located below the interface. Experiment running at  $b_o=400 \mu\text{m}$  and  $\omega=4.85 \text{ rad/s}$  (a) and  $\omega=5.39 \text{ rad/s}$  (b).

position was plotted against the angular frequency of the cylinder, for a given distance  $b_o$ , as shown in Fig. 3. This may be compared to a steady hydrodynamic model for this experiment developed in Ref. [14], which predicts the interface position in the straight morphology. It gives the interface recoil as a function of the angular frequency of the rotating cylinder as

$$x = \sqrt{2R_o b_o \left( \frac{2}{3F(\text{Ca})} - 1 \right)}, \quad (1)$$

where  $R_o$  is the cylinder radius and  $\text{Ca}$  is the capillarity number ( $\text{Ca} = \frac{\mu V}{T}$ ). The function  $F(\text{Ca})$  was used originally by Tabeling *et al.* [18] for the planar-to-planar geometry in order to describe wetting effects at the plates and it is given by

$$F(\text{Ca}) = c(1 - \exp\{-[d\mu R_o(\omega - \omega_o)/T]^{2/3}\}).$$

Except for very low frequencies, we obtained a good fit of Eq. (1) to our data of interface recoil. Typical data, for  $b_o=300 \mu\text{m}$ , is shown in Fig. 3. Even beyond the bifurcation point, Eq. (1) adjusts perfectly well to the mean interface position. At very low frequencies, insufficient wetting affects the establishment of a steady flow close to the cylinder and prevents the use of this hydrodynamic model. The parameters obtained are consistent with reported empirical values

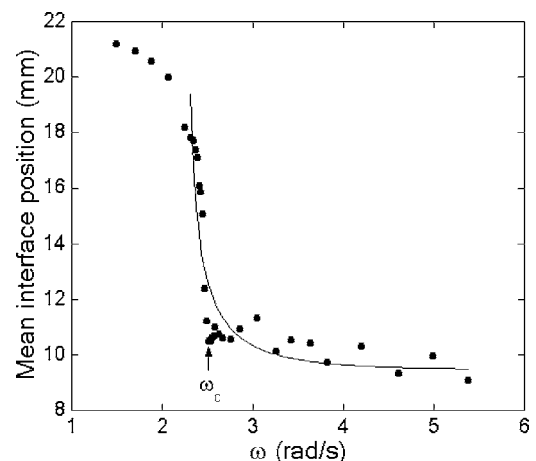


FIG. 3. Measured interface recoil (●) at various angular frequency for  $b_o=300 \mu\text{m}$ . Curve (line) adjusted by using the steady approximation [Eq. (1)]. The critical angular frequency is  $\omega_c$ . Obtained values for parameters of the function  $F(\text{Ca})$  at various distances  $b_o$  are  $b_o=300 \mu\text{m}$  ( $c=0.12$  and  $d=14.1$ ),  $b_o=400 \mu\text{m}$  ( $c=0.16$  and  $d=3.1$ ) and  $b_o=800 \mu\text{m}$  ( $c=0.20$  and  $d=2.1$ ).

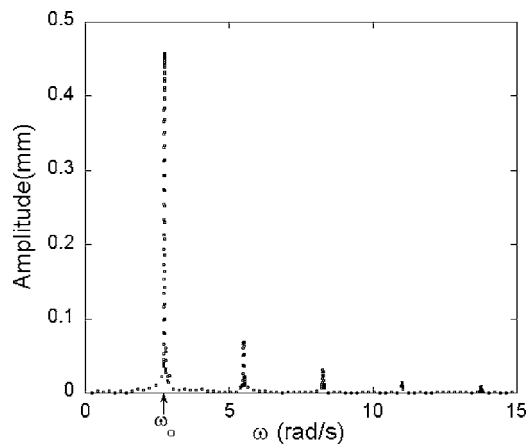


FIG. 4. Fourier spectrum of the interface oscillations. The presence of a strong peak at the angular frequency of the cylinder ( $\omega_o$ ) reveals that the eccentricity is the cause of observed interface oscillations. Data for  $b_o=300 \mu\text{m}$  and  $\omega=2.53 \text{ rad/s}$ .

and with the prescribed nominal values of  $b_o$  used in each experiment.

Due to cylinder eccentricity the distances  $b_o$  and the radius  $R_o$  vary in time as

$$\begin{aligned} b_o(t) &= b_o - \epsilon \sin(\omega t), \\ R_o(t) &= R_o + \epsilon \sin(\omega t). \end{aligned} \quad (2)$$

This eccentricity changes pressure and velocity fields of the fluid close to the cylinder. Consequently, the interface position oscillates at the same frequency of the cylinder. The effect is captured by the temporal Fourier transform of the mean interface position, which shows a strong peak at the angular frequency of the cylinder, as displayed in Fig. 4. The peak-to-peak intensity of this oscillation ( $\sim 920 \mu\text{m}$ ) is bigger than the eccentricity by two orders of magnitude. In order to characterize and analyze this phenomenon, careful measurements of the amplitude of this fundamental mode in both pre- and post-bifurcation branches were made. The data obtained shows that this amplitude grows critically as the bifurcation approaches. This is shown on the left-hand side of Fig. 5, for  $b_o=300 \mu\text{m}$ , where the Fourier amplitude is displayed as a function of the reduced control parameter,

$$\xi = \frac{\omega - \omega_c}{\omega_c}.$$

After the onset of periodic pattern mean interface position was still calculated as the arithmetic mean of extracted pixel data. The observations showed that the same oscillatory mode for this mean interface position still persisted. However, for large values of the control parameter, when the unstable spatial modes are nonlinear, the oscillations get suppressed. This may indicate that curvature effects could be important as a stabilizing mechanism of these oscillations. The overall effect, encompassing both pre- and post-bifurcation regions is displayed in Fig. 5. Although obtained in a different context, it is worthwhile to stress that a profile, similar to the one we observed in the prebifurcation branch,

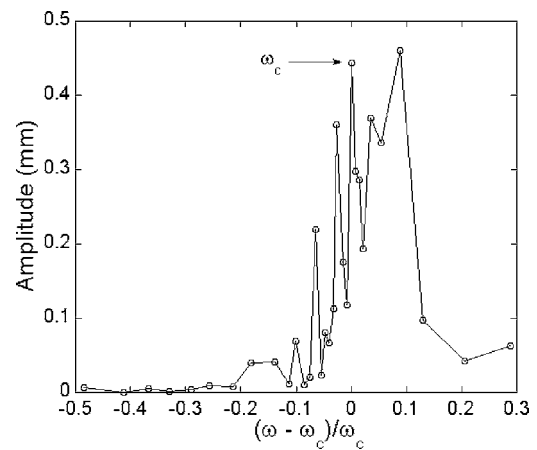


FIG. 5. Fundamental Fourier mode of the interface oscillations measured at different angular frequencies for  $b_o=300 \mu\text{m}$ . Lines are for a guide to the eye only and  $\omega_c$  is the critical angular frequency.

was reported by Martinerie *et al.* [6] and by Lehnertz and Elger [7], both for EEG data, showing the existence of precursors in epileptic seizures. These precursors were verified in nonlinear time-series analysis of EEG signal in different brain states but no detailed characterization was reported. The main feature of this analysis is centered on the amplification of a relevant variable before a bifurcation happens. This result is considered as a precursor for the type of phenomenon analyzed. The kind of phenomena studied in our work has a completely different origin since it comes from a deterministic perturbation in a controllable experiment. However, the profile of both curves, showing amplification of a relevant experimental variable prior to a bifurcation is an indication that really we observed a precursor in our experiments. In fact, for all values of  $b_o$ , strong variations of the fundamental Fourier peak were observed for small values of the control parameter at both pre- and post-bifurcation points. In order to obtain the profile of this set of data we applied a smoothing procedure by replacing each experimental point by an average of five adjacent points centered on the point under observation. This mean filter [19] cuts high frequency Fourier modes of the curve. The criteria used to select the number of adjacent points entered in the filter is the visual length of the fluctuations (the Nyquist frequency), which in almost all cases covers no more than three points. This determines the filtering window, measured as 2 times this length. The resulting effect of this mean filter is a reduction in the intensity variation between one experimental data and its adjacent neighbors. So, with this procedure it was possible to observe that an evident trend (locally monotonic) is always present in these profiles. The resulting curves are shown in Fig. 6 for different values of  $b_o$ . Notice that minimum amplitude of the fundamental Fourier mode may be smaller than one-half of the spatial resolution because some power is delivered to its harmonics.

Interesting features, concerning the character of the critical approach to the bifurcation point, result from the analysis of these filtered data. In the prebifurcation regime, the curves fit very well to a power law of the type

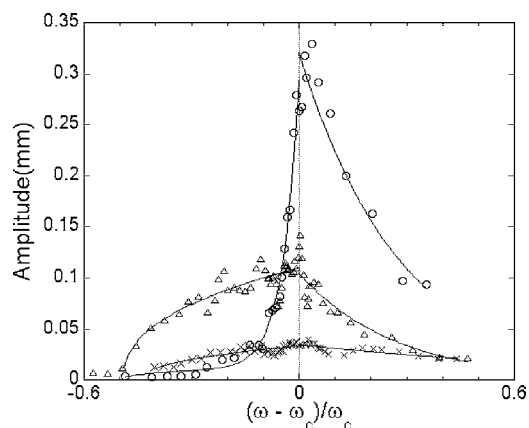


FIG. 6. Filtered data of the fundamental Fourier mode adjusted to a power law in the prebifurcation branch and to an exponential in the post-bifurcation branch. [( $\circ$ )  $b_o=300 \mu\text{m}$ ; ( $\Delta$ )  $b_o=400 \mu\text{m}$ ; ( $\times$ )  $b_o=800 \mu\text{m}$ ].

$$A = \alpha(\xi - \xi_a)^\beta. \quad (3)$$

After the bifurcation, this trend still persists in a small range of the control parameter. Then, it experiences an exponential decrease until the oscillations come close to the initial values observed in large negative values of the control parameter. The best fit between Eq. (3) and each experiment is depicted in Fig. 6 and the set of adjusted parameters is displayed in Table I. As already noticed, it is clear that the amplitude of interface oscillations is bigger than the eccentricity. But, what is more interesting and clearly evident is the nonanalytical character of the overall amplitude profile close to the bifurcation, where a cuspid is present and defined by a transition of the power law to an exponential trend. The existence of this cuspid as well as the persistent amplification after the bifurcation has been reported by Bryant *et al.* [20] in the study of Josephson junction parametric amplifiers, where a supercritical bifurcation is also observed. Moreover, in a large interval of the control parameter, located inside of the prebifurcation branch, two different types of critical approach to the bifurcation point were observed. For the largest value of  $b_o$ , the critical exponent  $\beta$  is smaller than one. In order to adjust data corresponding to the smallest  $b_o$ , combination of two functions like those in Eq. (3) was used. In one of them we used the same parameters as before. It describes an initial low amplitude trend. The other one, describes the strong amplification observed close to the bifurcation point,

TABLE I. Values of parameters obtained by adjusting a power law [Eq. (3)] to experimental data. The errors for exponent  $\beta$  and correlation coefficient  $R$  are shown. Values labeled with an asterisk (\*) are maintained constant in the fitting procedure.

Distance $b_o(\mu\text{m})$	$\alpha$	$\xi_a$	$\beta$	$R$
800	0.05	-0.44	$0.45 \pm 0.14$	0.88
400	0.15	-0.49	$0.42 \pm 0.05$	0.90
300	0.25	-1.01	$21.46 \pm 1.21$	0.99
	$0.02^*$	$-0.50^*$	$0.43^*$	

presenting an exponent as large as 21 (see Table I). It seems that both cases are also pictured for the intermediate value of  $b_o=400 \mu\text{m}$  in which a climbing cuspid, located very close to the bifurcation point, seems to be superimposed over the extended and flat profile dominant in the prebifurcation branch. Another important feature, clear from the type of power law used in Eq. (3), is the existence of a point, defined by the parameter  $\xi_a$  (the “anticipating” control parameter), above which the interface becomes oscillatory. Consequently, a closed interval of the control parameter  $\xi \in [\xi_a, \xi_c]$  located inside of the high symmetry branch and adjacent to the bifurcation point may be defined. The existence of this interval, the “precursor branch,” determines whether the dynamics of the homogenous state is sensitive to the bifurcation or not. Thus, a new branch has been described possessing an entirely different origin compared to usual bifurcation points obtained from linear stability analysis, which shows the emergence of the pattern formation.

It is now important to determine if the available theoretical models may account for the existence of this precursor branch as consequence of a trivial response of the system to the imposed perturbation. In this respect, the immediate effect demanding explanation is the observed hydrodynamic gain, defined by the ratio of the peak-to-peak interface oscillation to eccentricity. A likely explanation for this effect could be a passive adjustment of the hydrodynamic fields, calculated by the quasisteady approximation to eccentricity. In order to check this possibility, we introduced in Eq. (1) the perturbation described by Eqs. (2) and calculated the corresponding maximum variation range of the interface position. The resulting equation is

$$\Delta x = \epsilon \sqrt{\frac{R_o}{b_o} \left( \frac{2}{3F(\text{Ca})} - 1 \right)}. \quad (4)$$

It was not included in this formula the variations in the capillarity number induced by eccentricity because their effect on the function  $F(\text{Ca})$  is small (about 0.5%). The formula displayed in Eq. (4) correctly predicts an oscillating interface at the same frequency as the rotating cylinder and a hydrodynamic gain given by  $\sqrt{\frac{R_o}{b_o}}$ , which qualitatively explains the measured values obtained. However, it is unable to describe the observed prebifurcation trend of the oscillations, for it predicts a decreasing peak intensity given as a function of the cylinder frequency. This indicates that the perturbation couples to the hydrodynamic fields through effects that are not trivial. The possibility of a Hopf bifurcation at zero wave vector  $\mathbf{k}$  must also be considered. However, the growth rate of spatial modes, obtained from the linear stability analysis of interface morphology [14], does not predict imaginary values for any  $\mathbf{k}$ . Consequently, a Hopf bifurcation at  $\mathbf{k}=\mathbf{0}$  may not exist in the prebifurcation branch. Therefore, the absence of a Hopf bifurcation and the failure of the steady hydrodynamic theory in explaining the perturbed prebifurcation profile imply that the oscillations of the interface are determined by the whole set of dynamical interactions in the nonequilibrium thermodynamic fields and variables relevant to the experiment. This conclusion supports our argument that eccentricity induces dynamical effects in the prebifurca-



tion branch, which manifest in the interface dynamics as critical prebifurcation oscillations of interface position. Therefore, a precursor was in fact observed. Its existence is hidden in the steady theory of interface position when calculated by using the geometry of a perfect cylinder, consistent with any reasonable values of  $b_o$  and  $R_o$ . It may account only for constant values of these variables but may not give support to any additional dynamics induced by a time-dependent perturbation generated by eccentricity.

In conclusion, the present work reports the observation of a type of precursor, induced by a deterministic time-dependent perturbation acting over a high symmetry branch, while preserving the pattern structure of this branch. In this sense, a time-domain pattern signals in advance the existence of a post-bifurcation branch presenting a spatial pattern. So far, reported precursors, mainly those excited by an external noise source, generate prebifurcation spurious spectra which signals the existence of post-bifurcation modes. In the

present case, it seems that no information concerning the post-bifurcation state is present, at least in the form of a direct determination of the selected pattern. The immediate information concerns only the emergence of a bifurcation. However, the existence of an anticipating control parameter and critical exponents indicate the action of hidden dynamics, not accounted for in the linear stability analysis of the interface morphology. Thus, the verification that the amplitude of the prebifurcation oscillations we observed, follows a power law, might indicate that a universality class for this phenomena exists. This observation justifies further studies on the detection of precursory activities and the need of precise monitoring close-to-bifurcations regimes in complex systems.

This work was partially supported by Brazilian Agencies: CNPq and Finep-Pronex.

- 
- [1] K. Wiesenfeld, *J. Stat. Phys.* **38**, 1071 (1985).
  - [2] *Evaluation of Proposed Earthquake Precursors*, edited by M. Wyss (American Geophysical Union, Washington, DC, 1991).
  - [3] M. Wyss, *Pure Appl. Geophys.* **149**, 3 (1997).
  - [4] K. Eftaxias, P. Kaporis, J. Polygiannakis, A. Peratzakis, J. Kapanas, G. Antonopoulos, and D. Rigas, *Nat. Hazards Earth Syst. Sci.* **3**, 217 (2003).
  - [5] P. E. McSharry, L. A. Smith, L. Tarassenko, J. Martinerie, M. Le Van Quyen, M. Baulac, and B. Renault, *Nat. Med.* **9**, 241 (2003).
  - [6] J. Martinerie, C. Adam, M. Le Van Quyen, M. Baulac, S. Clemenceau, B. Renault, and F. J. Varela, *Nat. Med.* **4**, 1173 (1998).
  - [7] K. Lehnertz and C. E. Elger, *Phys. Rev. Lett.* **80**, 5019 (1998).
  - [8] C. Jeffries and K. Wiesenfeld, *Phys. Rev. A* **31**, 1077 (1985).
  - [9] H. Lamela, S. Prez, and G. Carpintero, *Opt. Lett.* **26**, 69 (2001).
  - [10] K. Wiesenfeld and B. McNamara, *Phys. Rev. A* **33**, 629 (1986).
  - [11] K. Wiesenfeld and N. F. Pedersen, *Phys. Rev. A* **36**, 1440 (1987).
  - [12] E. D. Surovyatkina, *Phys. Lett. A* **329**, 169 (2004).
  - [13] Y. A. Kravtsov and E. D. Surovyatkina, *Phys. Lett. A* **319**, 348 (2003).
  - [14] V. Hakim, M. Rabaud, H. Thomé, and Y. Couder, in *Proceedings of a NATO Advanced Research Workshop: New Trends in Nonlinear Dynamics and Pattern Forming Phenomena: The Geometry of Nonequilibrium*, edited by P. Couillet and P. Huerre (Plenum, New York, 1990), p. 237.
  - [15] E. Pitts and J. Greiller, *J. Fluid Mech.* **11**, 33 (1961).
  - [16] M. Rabaud, S. Michalland, and Y. Couder, *Phys. Rev. Lett.* **64**, 184 (1990).
  - [17] H. Z. Cummins, L. Fournet, and M. Rabaud, *Phys. Rev. E* **47**, 1727 (1993).
  - [18] P. Tabeling, G. Zocchi, and A. Libchaber, *J. Fluid Mech.* **177**, 67 (1987).
  - [19] R. C. Gonzales and R. E. Woods, *Digital Image Processing*, 2nd ed. (Pearson Education, Delhi, 2002).
  - [20] P. Bryant, K. Wiesenfeld, and B. McNamara, *J. Appl. Phys.* **62**, 2898 (1987).